

# Assessing the Integration of Total Least Squares and Radial Basis Function Neural Network for Coordinate Transformation

<sup>1</sup>Bernard KUMI-BOATENG, <sup>1</sup> Joseph Edem VIGBEDOR

<sup>1</sup>Faculty of Geosciences and Environmental Studies, Department of Geomatic Engineering, University of Mines and Technology, Tarkwa, Ghana.

Corresponding authors: kumi@umat.edu.gh; josephedem2012@gmail.com

## Abstract

*Total Least Squares (TLS) is noted to be a solution approach to solving several geodetic problems. The method has the ability to estimate unknown quantities that are useful for many geodetic applications. Hence, the main objective of this study is to improve the estimation performance of TLS via Radial Basis Function Neural Network (RBFNN) in coordinate transformation. This hybrid approach called TLS-RBFNN was applied to Ghana geodetic reference network, which has a coverage area of 79857 km<sup>2</sup> representing 33.5% of the total land mass (238540 km<sup>2</sup>). A comparative performance analysis of TLS, RBFNN and TLS-RBFNN was carried out using Root Mean Square Horizontal Error (RMSHE) and Standard Deviation (SD). Based on the testing results, it was found that the TLS-RBFNN improved the transformation accuracy of RBFNN and TLS by 20.240% and 37.240% based on the RMSHE. In addition, it was observed that the TLS-RBFNN improved the transformation precision based on SD by 0.3703% and 8.52%, respectively. Furthermore, the Bayesian Information Criterion (BIC) applied confirmed the superiority of the hybrid approach than using TLS and RBFNN as independent transformation methods. Consequently, the hybrid approach is recommended for enhanced coordinate transformation results in Ghana geodetic reference network.*

**Keywords:** Total Least Squares, Artificial Neural Network, Coordinate Transformation, Global Navigation Satellite System

---

Assessing the Integration of Total Least Squares and Radial Basis Function Neural Network for Coordinate Transformation (11905)  
Bernard Kumi-Boateng and Joseph Edem Vigbedor (Ghana)

FIG Working Week 2023  
Protecting Our World, Conquering New Frontiers  
Orlando, Florida, USA, 28 May–1 June 2023

## INTRODUCTION

Global Navigation Satellite System (GNSS) has been a major source of technology used for Earth observations since its inception. GNSS, particularly Global Positioning System (GPS), has become increasingly popular over the years, due partly to the multitude of problems associated with the conventional surveying techniques. It is well acknowledged that GNSS acquired data is based on geocentric system of reference and thus cannot be directly used in astro-geodetic datums. Hence, due to change in datum position, size and shape, coordinate transformation between two geodetic datums qualifies it to be a good choice. Thus, the transformation attempts to provide a unifying approach that bridges the gap between the different datums.

Several conventional transformation methods such as Bursa-Wolf (Bursa, 1962; Wolf, 1963), Molodensky-Badekas (Molodensky, Yeremeyev, & Yurkina, 1962; Badekas, 1969), geocentric translation model, standard Molodensky, Abridged Molodensky, polynomial and multiple regression (Applebaum, 1982; Featherstone, 1997; Fraser and Yamakawa, 2004; Newsome and Harvey, 2003) have been widely applied in literature. These mentioned techniques have peculiar characteristics they have been employing to accomplish the coordinate transformation tasks. Thus, by utilising set of transformation parameters.

Over the years, numerous techniques have been proposed and used to determine the transformation parameters. In practice, the most common alternatives may be categorised into least squares algorithms, partitioning methods, Ill-posed approach, quaternions approach and Procrustes algorithm (Collier, Argeseanu, & Leahy, 1998; Soler and Snay, 2003; Grafarend and Awange, 2003; Shen, Chen, & Zheng, 2006; Felus and Schaffrin, 2005; Lippus, 2004). However, the popularity of Artificial Neural Network (ANN) methodology has been growing in a wide variety of areas in geodesy and geomatic engineering. Its efficacy as a coordinate transformation technique is well documented. Literature confirms that the ANN approaches could produce reasonable and promising results that are more satisfactory than the empirical affine, conformal and projective transformation methods (Tierra, De Freitas, & Guevara, 2009; Kumi-Boateng and Ziggah, 2017; Ziggah, Youjian, Tierra, Konaté, & Hui, 2016a;

Ziggah, Youjian, Yu, & Laari, 2016b; Ziggah, Youjian, Laari, & Hui, 2017; Ziggah, Issaka, Laari, & Hui, 2018; Ziggah, & Laari, 2018; Ziggah, Youjian, Tierra, & Laari, 2019a; Ziggah, Hu, Issaka, & Laari, 2019b; Gullu and Narin, 2019 and references therein). The strength of the ANN has been credited to its ability to effectively reduce the distortion and heterogeneity in spatial data related to the different geodetic datums. Moreover, the self-adaptive feature of the ANN enables it to appropriately identify hidden patterns in a data set to build the prediction model.

In the last few years, combining ANN and empirical methods to create a hybrid approach is becoming very popular among geoscience researchers. Examples of some application areas include landslide studies (Huang, Wu, & Ziggah, 2016 and references therein), hydrological studies (Tiwari, Adamowski, & Adamowski, 2016 and references therein), meteorology (Ghorbani, Khatibi, Fazeli Fard, Naghipour, L., & Makarynsky, 2016 and references therein) to mention but a few. Literature reveals that the hybrid approach offers better computational efficiency than separately applying the methods. Whereas the hybrid concept is becoming much appreciated, none of the existing studies in coordinate transformation fully address the issue of combining empirical transformation procedure and ANN technique or any other soft computing techniques. The dominance of ANN to solve several geodetic problems (e.g. coordinate transformation, tide modelling, gravity field modelling, orbit determination, digital terrain height estimation, crustal deformation, GNSS error modelling, etc.) makes it important computational tool (Tierra and De Freitas, 2005; Kaftan, Salk, & Senol, 2011; Liao, Wang, Zhou, Liao, & Huang, 2012; Salim, Dwarakish, Liju, Thomas, Devi, & Rajeesh, 2015; Lei, Zhao, Cai, 2015; Okwuashi and Ndehedehe, 2015; Huang et al., 2016; Razin and Voosoghi, 2017; Gullu and Narin, 2019).

Therefore, motivated by the successful application of ANN, the main focus of this study is to explore the potential of integrating Total Least Squares (TLS) and Radial Basis Function Neural Network (RBFNN) in coordinate transformation process. **The choice of these methods was based on its frequent use, simplicity in application and computational efficiency.** The TLS-RBFNN integrated approach was tested in Ghana geodetic reference network to perform

coordinate transformation between the global WGS84 and Ghana's War Office 1926 ellipsoid. Such integration approach is significant for Ghana because of the astro-geodetic datum used for surveying and mapping works. In addition, with all the attendant problems of the astro-geodetic datums in mind (see Varga, Grgić, & Bašić, 2017; Poku-Gyamfi, 2009), the need to explore and test the potential of different coordinate transformation procedures in the Ghana geodetic reference network is reasonable. In continuance of that, the TLS and RBFNN when combined will both use their strengths and weaknesses to complement each other. Thus, the hybrid approach will combine their function approximation and nonlinear modelling capabilities.

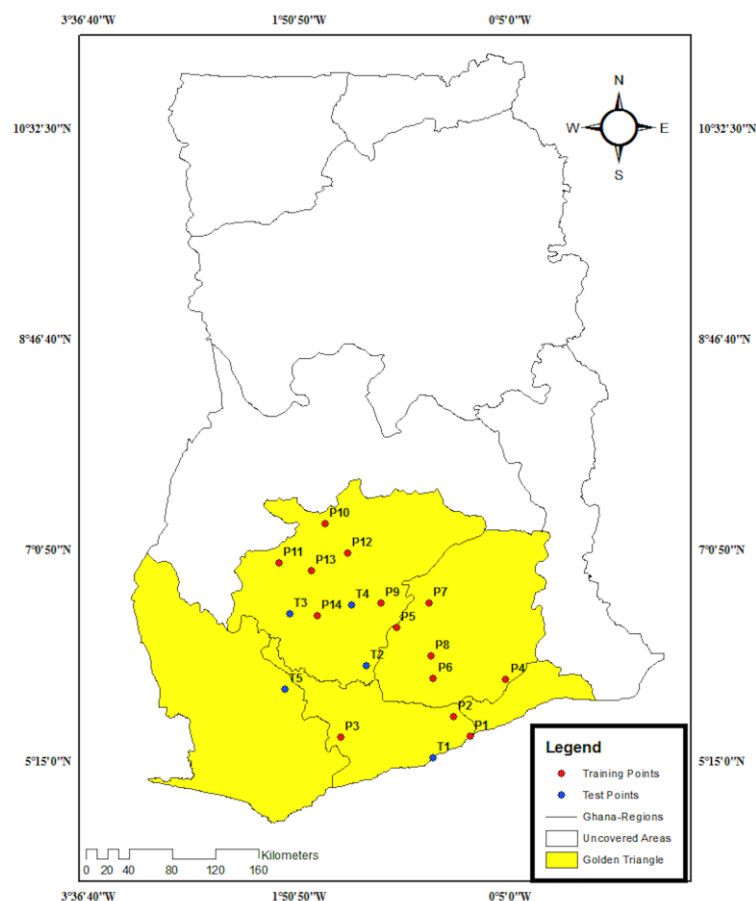
Moreover, using TLS can improve the performance of the RBFNN in many aspects such as training speed, reduction in the size of the network leading to fast convergence and satisfactory transformation results. The proposed hybrid approach could be categorised as a combination of knowledge-based system and empirical model. The idea behind this study is not to take away the significance of the empirical transformation models, but to demonstrate from a practical perspective how combining those with ANN can be more effective in solving coordinate transformation problems. Evidently, this study shows the potential and the resulting consequences of using such hybrid approach as a practical tool for coordinate transformation in Ghana geodetic reference network.

## MATERIALS AND METHODS

### Study Area and Data Used

Ghana is a West African country bounded by latitudes 4°30' N and 11° N, and longitudes 3° W and 1° E (Mugnier, 2000). The country uses the Accra 1929 datum for its geospatial activities. The reference ellipsoid of the Accra 1929 datum is the War Office 1926. This reference ellipsoid has its origin at latitude 5° 23' 43.33" N and longitude 0° 11' 52.3" W with semi-major axis  $a = 6378299.99899832$  m, semi minor axis  $b = 6356751.68824042$  m and inverse flattening  $f = 296$  (Poku-Gyamfi, 2009; Ayer, 2008; Ayer and Fosu, 2008). For the purposes of land surveys, the Transverse Mercator projection has been adopted to derive projected grid coordinates in Easting and Northing. The Transverse Mercator has its origin at

longitude  $01^{\circ} 00' W$  and latitude  $04^{\circ} 40' N$  with false Easting value of 274319.736 m added to all Y coordinates to avoid negative coordinates and setting the false Northing to zero (Mugnier, 2000; Poku-Gyamfi, 2009). A used scale factor of 0.99975 was found to eliminate the scale distortion effect within the country but this can exceed the projection values only at the borders (extreme ends) of the country. Since Accra 1929 datum is non-geocentric but GPS acquired data based on WGS84 is geocentric, localisation of the GPS data will require coordinate transformation. In this study, two sets of 19 co-located points were collected based on the War Office 1926  $(\varphi, \lambda, h)_{WAR}$  and WGS84  $(\varphi, \lambda, h)_{WGS84}$ ; where  $\varphi$  is the geodetic latitude,  $\lambda$  is the geodetic longitude and  $h$  is the ellipsoid height. The point distribution of the data used for the analysis is shown in Figure 1. These data sets were provided by the Ghana Survey and Mapping Division of Lands Commission from the Land Administration Project. It is important to note that these co-located points are the only available data set and those for the northern part and the rest of the country are yet to be observed.



Assessing the Integration of Total Least Squares and Radial Basis Function Neural Network for Coordinate Transformation (11905)

Bernard Kumi-Boateng and Joseph Edem Vigbedor (Ghana)

FIG Working Week 2023

Protecting Our World, Conquering New Frontiers

Orlando, Florida, USA, 28 May–1 June 2023

**Figure 1.** Co-Located Points Distribution in the Study Area

## APPLIED METHODS

### Total Least Squares

The generic least squares type is the Ordinary Least Squares (OLS) with the implicit assumption that the errors in the design matrix are zero but the only errors present can be found in the observation vector. However, in geodetic practice, all observed data (coordinates) may suffer some form of errors. In order to correct for such errors, a more pragmatic TLS approach is needed (Felus and Schaffrin, 2005; Akyilmaz, 2007; Okwuashi and Eyoh, 2012). Consequently, this study applied the TLS approach for the coordinate transformation due to its superiority to the OLS in producing precise coordinate transformation results as indicated by several authors (Akyilmaz, 2007; Felus and Schaffrin, 2005; Okwuashi and Eyoh, 2012).

Golub and Van Loan (1980) introduced the TLS approach as a solution technique to estimate an over-determined system of linear equations expressed in Equation (1) as

$$BX = K \quad (1)$$

where  $B \in R^{m \times n}$  and  $K \in R^{m \times d}$  are the given datasets,  $X \in R^{n \times d}$  is the unknown parameters to be determined,  $m$  is the number of observations,  $n$  is the number of unknowns and  $m \geq n$ . To estimate  $X$  in Equation (1), the design matrix ( $B$ ) is considered to be affected by random errors expressed in Equation (2) (Akyilmaz, 2007) as

$$(B + v_B)X = K + v_K, \text{rank}(B) = m < n \quad (2)$$

It must be known that both  $v_K$  (error vector of observations) and  $v_B$  (error matrix of data matrix) in Equation (2) are presumed to have independent and equivalent distributed rows with zero mean and equal variance (Akyilmaz, 2007). To minimize the errors in the data, the TLS approximation (Equation 3) is iteratively applied.

$$\min \left\| \begin{bmatrix} B; K \end{bmatrix} - \begin{bmatrix} \hat{B}; \hat{K} \end{bmatrix} \right\|_F, \begin{bmatrix} \hat{B}; \hat{K} \end{bmatrix} \in R^{m \times (n+1)}, \text{subject to: } \hat{K} \in R(\hat{B}) \quad (3)$$

where  $m$  and  $n$  are the same as defined in Equation (1);  $\hat{B}$  is the new estimated data matrix;  $\hat{K}$  is the new estimated observation vector; and  $\| \cdot \|_F$  is the Frobenius norm of  $m \times n$  matrix.

Equation (3) iteration continues until a minimizing matrix  $\begin{bmatrix} \hat{B}; \hat{K} \end{bmatrix}$  is found such that any  $\hat{X}$  (estimated unknown parameters) satisfying  $\hat{B}\hat{X} = \hat{K}$  is the TLS solution and  $\begin{bmatrix} \Delta\hat{B}; \Delta\hat{K} \end{bmatrix} = \begin{bmatrix} B; K \end{bmatrix} - \begin{bmatrix} \hat{B}; \hat{K} \end{bmatrix}$  is the corresponding TLS correction (Akyilmaz, 2007; Golub and Van Loan, 1980; Okwuashi and Eyoh, 2012). It is worth mentioning that the TLS solution is usually determined through the functional relation expressed in Equation (4) as

$$\begin{bmatrix} B; K \end{bmatrix} \begin{bmatrix} \hat{X}^T; -1 \end{bmatrix}^T \approx 0. \quad (4)$$

In this study, the Singular Value Decomposition (SVD) approach was applied on the matrix  $\begin{bmatrix} B; K \end{bmatrix}$  to solve the TLS problem. Using the SVD enables the matrix  $\begin{bmatrix} B; K \end{bmatrix}$  to be investigated to know whether it is rank deficient or not. The SVD mathematical representation of the matrix  $\begin{bmatrix} B; K \end{bmatrix}$  (Van Huffel and Vandewalle, 1991) is given in Equation (5) as

$$\begin{bmatrix} B; K \end{bmatrix} = USV^T \quad (5)$$

where  $U = [U_1; U_2]$ ,  $U_1 = [u_1, \dots, u_n]$ ,  $U_2 = [u_{n+1}, \dots, u_m]$ ,  $u_i \in R^m$ ,  $U^T U = I_m$ ,

$$V = \begin{bmatrix} V_{11} & V_{12} \\ V_{21} & V_{22} \end{bmatrix}_d^n = [v_1, \dots, v_{n+d}] v_i \in R^{n+d}, V^T V = I_{n+d},$$

$$S = \begin{bmatrix} \Sigma_1 & 0 \\ 0 & \Sigma_2 \end{bmatrix} = \text{diag}(\sigma_1, \dots, \sigma_{n+1}) \in R^{m \times (n+d)}, t = \min\{m-n, d\},$$

$$\Sigma_1 = \text{diag}(\sigma_1, \dots, \sigma_n) \in R^{n \times n},$$

$$\Sigma_2 = \text{diag}(\sigma_{n+1}, \dots, \sigma_{n+t}) \in R^{(m-n) \times d}, \text{ and } \sigma_1 \geq \dots \geq \sigma_{n+1} \geq 0.$$

The  $\sigma_i$  are the singular values of  $B$  and  $\begin{bmatrix} B; K \end{bmatrix}$ , and the vectors  $u_i$  and  $v_i$  are the  $i$ th left and right singular vector of  $B$  and  $\begin{bmatrix} B; K \end{bmatrix}$ , respectively. A TLS solution exists if and only if  $V_{22}$  is non-singular and the solution is unique if and only if  $\sigma_n \neq \sigma_{n+1}$ . The TLS solution is therefore expressed as  $\hat{X}_{tls} = -V_{12} V_{22}^{-1}$  and the corresponding TLS correction matrix is expressed in Eq. (6) as

$$\Delta C_{TLS} = [\Delta B_{TLS}; \Delta K_{TLS}] = -U \text{diag}(0, \Sigma_2) V^T. \quad (6)$$

**Radial Basis Function Neural Network**

Broomhead and Lowe (1988) proposed RBFNN technique which processes information by using norms and radial basis functions. This network creates an alternative means of applying arbitrary input-output patterns for function approximation problems (Deyfrus, 2005). It has a feedforward topology consisting of three layers; the input, hidden and output that are completely linked together. Figure 2 shows the RBFNN architecture with inputs ( $X_1, X_2, \dots, X_d$ ), radial basis function ( $\varphi_1, \varphi_2, \dots, \varphi_N$ ), weight ( $W_1, W_2, \dots, W_N$ ) and output ( $y$ ) respectively.

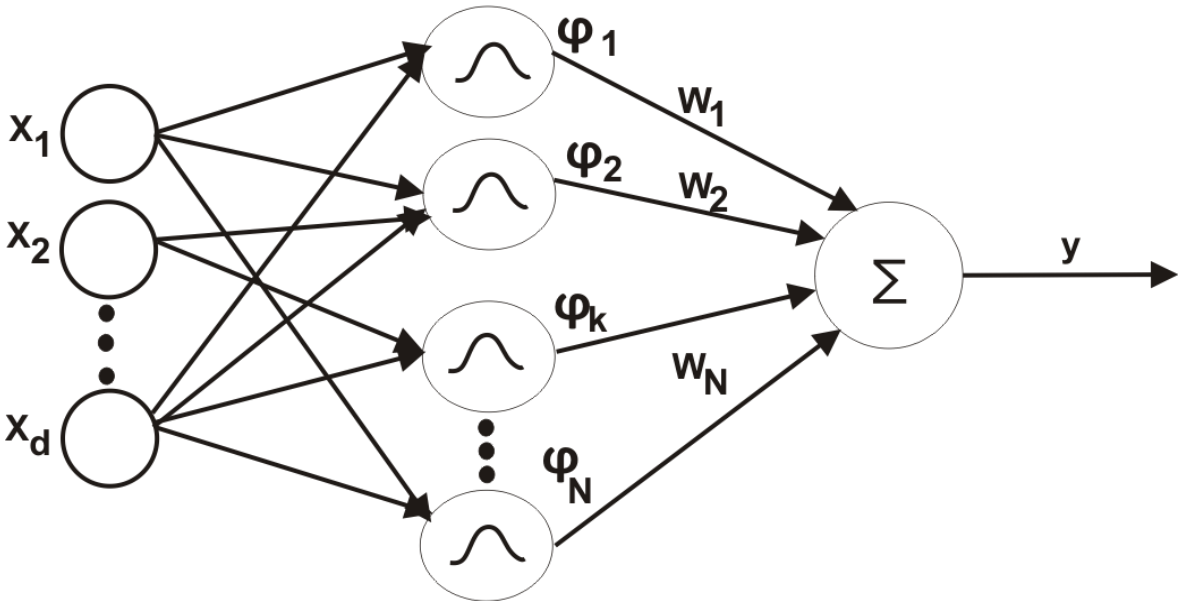


**Figure 2.** RBFNN Structure

This study adopted the supervised learning algorithm to train the RBFNN. A code written in MATLAB environment was used to carry out the RBFNN training. In the RBFNN scheme, the input layer comprises the data that are submitted into the network by unweighted connections. These input nodes are then transmitted into the hidden layer chamber by a non-linear activation function. Within the hidden layer, each neuron computes a Euclidean norm that represents the distance between the input to the network and the position of the neuron

called the centre. This is then inserted into a radial basis transfer function which estimates and outputs the activation of the neuron (Deyfrus, 2005). This study applied the Gaussian activation function expressed in Equation (7) as

$$\beta_i(X) = \exp \left[ -\frac{\|X - \mu_j\|^2}{2\sigma_i^2} \right] \quad (7)$$

where  $\beta_i(X)$  denote the hidden layer output of the  $i$ th unit,  $X$  is the input vector,  $\mu_j$  is the centre of the Gaussian function for the hidden node  $j$ ,  $\sigma_i$  is a spread parameter for regulating smoothness properties of the Gaussian function and  $\|X - \mu_j\|$  is the Euclidean norm. When calculations are completed, the output layer containing the identity activation function then uses the weighted sum of the radial basis function layer as propagation function. The estimated output layer results from the RBFNN could be represented by Equation (8) (Jain, Singh, & Srivastava, 2011) as

$$y = \sum_{i=1}^M w_i \beta_i(X) + w_o, \quad (8)$$

where  $M$  is the number of radial basis function and  $w$  represent the weight of the network. The mean squared error (MSE) for the  $X$ th data was estimated using Equation (9) (Jain *et al.*, 2011).

$$MSE = \frac{1}{2} (y_o - y_p)^2 \quad (9)$$

where  $y_o$  and  $y_p$  are the actual output and target for the  $X$ th data, respectively. The training process was then repeated for all training data. Equation (10) (Jain *et al.*, 2011) was applied to estimate the error function ( $E_k$ ).

$$E_k = \sum_{X=1}^{X^{total}} MSE = \frac{1}{2} \sum_{X=1}^{X^{total}} (y_o - y_t)^2 \quad (10)$$

where  $X^{total}$  represents the total number of training data. The connection weight,  $w_{pi}$  which minimizes  $E_k$  was updated using Equation (11).

$$w_{pi}(K+1) = w_{pi}(K) + \Delta w_{pi}(K) \quad (11)$$

where  $\Delta w_{pi}(K)$  is given by Equation (12) as

$$\Delta w_{pi}(K) = \eta(K) \sum_{X=1}^{X^{total}} \delta_X A_{Xi} + \alpha \Delta w_{pi}(K-1). \quad (12)$$

where  $\eta(K)$  is the learning rate at  $K$ th iteration,  $\delta_X$  is the error signal of the  $X$ th data,  $\alpha$  is the momentum parameter and  $A_{Xi}$  denote the output vector of the hidden layer neuron  $i$  for all the input data. This RBFNN training process was repeated till the network error reaches an acceptable value.

### **Proposed Hybrid Model**

Local geodetic networks are highly distorted compared to the geocentric reference systems. The distortion is partly contributed by the conventional surveying techniques such as triangulation, traversing, resection and astronomical observations used in establishing the local geodetic network. Thus introducing distortions, systematic or observational errors within the network. Furthermore, the adjustment procedures used to adjust the local geodetic networks were of lower accuracies (see Varga *et al.*, 2017 and references therein). This supports the point made in Featherstone (1997) and Grgić, Varga, & Basic (2015) that the present conformal transformation models often times are unable to accurately reduce the distortion effects on the final transformation outputs.

After careful review of existing research works pertaining to Ghana geodetic network, the author realised that in many applications of the conformal transformation models, large residuals are often produced. Hence, in this study an attempt has been made to explore the integration of TLS and RBFNN in the transformation process. The motive is to determine the viability of such integrated approach for coordinate transformation in Ghana. Figure 3 denotes a summary of the proposed hybrid approach.

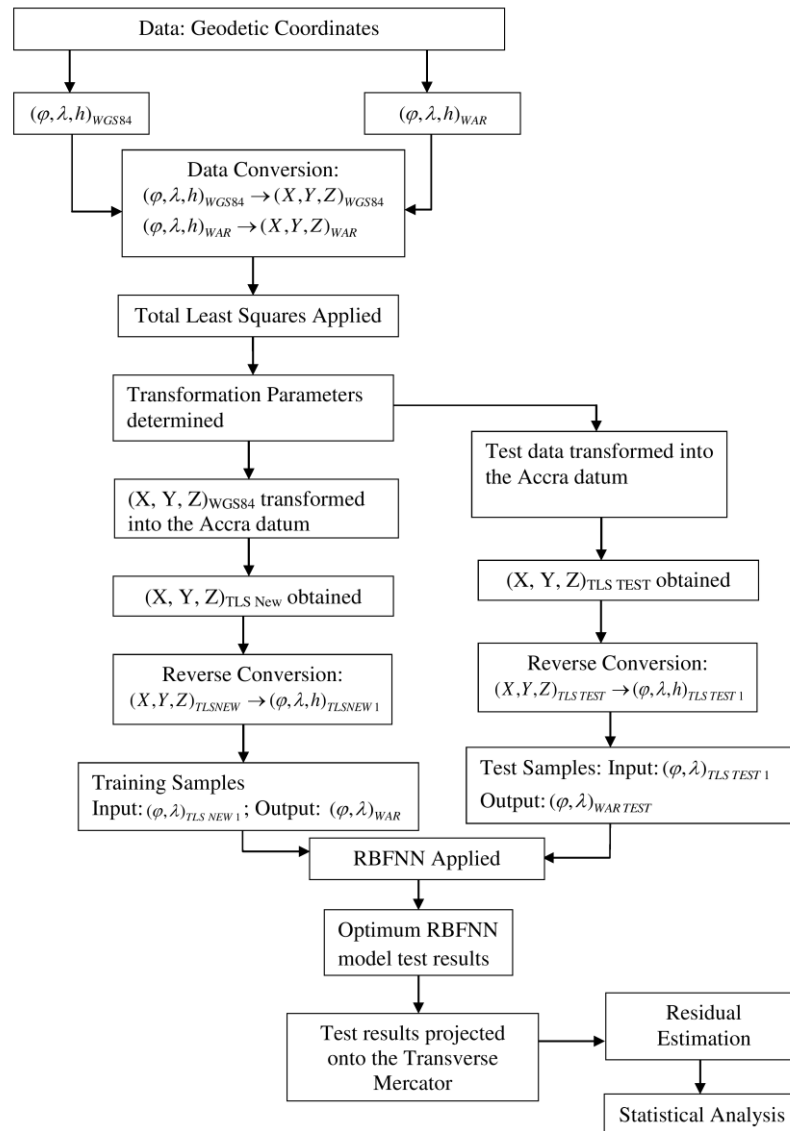


**Figure 3.** Flow Chart of the Proposed Hybrid Approach

Specific detail on how the hybrid approach was developed and implemented is presented as follows:

*Step 1: Converting Geodetic Coordinates to Cartesian Coordinates*

The geodetic coordinates of co-located points in both WGS84  $(\varphi, \lambda, h)_{WGS84}$  and War Office 1926  $(\varphi, \lambda, h)_{WAR}$  were converted into Cartesian coordinates using Equation (13) (Hofmann-

Wellenhof and Moritz, 2006). The results from Equation (13) for the WGS84 and War Office 1926 are designated in this study as  $(X, Y, Z)_{\text{WGS84}}$  and  $(X, Y, Z)_{\text{WAR}}$ , respectively.

$$\begin{aligned} X &= (S + h) \cos \varphi \cos \lambda \\ Y &= (S + h) \cos \varphi \sin \lambda \\ Z &= [S(1 - e^2) + h] \sin \varphi \end{aligned}$$

(13)

where  $S$  is the radius of curvature in the prime vertical as defined in Equation (14).

$$S = \frac{a}{\sqrt{1 - e^2 \sin^2 \varphi}} \quad (14)$$

$a$  and  $e$  are the semi-major axis and first eccentricity of the reference ellipsoid.

### *Step 2: Determine Coordinate Transformation Parameters*

Out of the 19 co-located points, 14  $(X, Y, Z)_{\text{WGS84}}$  and  $(X, Y, Z)_{\text{WAR}}$  were purposefully chosen as reference points set defined as  $P = (P_1, P_2, \dots, P_{14})$ . These points were applied to determine the transformation parameters for transforming WGS84 coordinates into Ghana War Office 1926. The remaining five points served as the independent reference test set defined as  $T = (T_1, T_2, \dots, T_5)$  for the model validation (see Figure 1). The seven parameter Bursa-Wolf (Bursa, 1962; Wolf, 1963) transformation model (Equation 15) was applied. It is known that for 14 common points, 35 observation equations more than the seven unknown parameters to be estimated. This clearly creates an over-determined system of linear equations. The TLS technique can be applied to such situations to achieve the best estimates of the unknown parameters. Hence, the TLS procedure based on the Singular Value Decomposition (SVD) approach (Equation 5) was applied to Equation (15) to determine the unknown transformation parameters. These determined parameters consisted of three translation vectors, three rotational parameters and one scale factor.

$$\begin{bmatrix} X_{\text{WAR}} \\ Y_{\text{WAR}} \\ Z_{\text{WAR}} \end{bmatrix} = \begin{bmatrix} T_X \\ T_Y \\ T_Z \end{bmatrix} + \eta R \begin{bmatrix} X_{\text{WGS84}} \\ Y_{\text{WGS84}} \\ Z_{\text{WGS84}} \end{bmatrix} \quad (15)$$

where  $T_X$ ,  $T_Y$  and  $T_Z$  are the translation vectors along X-, Y- and Z-axes respectively of the two reference systems.  $\eta$  is the scale factor and  $R$  is the total rotational matrix (product of the rotation angles).

### *Step 3: Apply the Determined Transformation Parameters*

The seven transformation parameters determined in Step 2 were then used to transform the 14 (X, Y, Z)<sub>WGS84</sub> into the War Office 1926 datum. These newly transformed Cartesian coordinates are denoted in this study as (X, Y, Z)<sub>TLS NEW</sub>. Similarly, the transformation parameters were also applied to transform the five independent test points into War Office 1926 datum. These transformed test coordinates are represented in this work as (X, Y, Z)<sub>TLS TEST</sub>.

### *Step 4: Convert Cartesian Coordinates to Geodetic Coordinates*

The (X, Y, Z)<sub>TLS NEW</sub> and (X, Y, Z)<sub>TLS TEST</sub> obtained in Step 3 were then converted to geodetic coordinates using Bowring inverse method (Equations 16-18) (Bowring, 1976). The converted coordinates were denoted in this study as  $(\varphi, \lambda, h)_{TLS\ NEW\ 1}$  and  $(\varphi, \lambda, h)_{TLS\ TEST\ 1}$ , respectively.

$$\varphi = \tan^{-1} \left[ \frac{Z + \varepsilon^2 b \sin^3 \xi}{p - e^2 a \cos^3 \xi} \right] \quad (16)$$

$$\lambda = \tan^{-1} \left[ \frac{Y}{X} \right] \quad (17)$$

$$h = p \cos \varphi + Z \sin \varphi - a \sqrt{1 - e^2 \sin^2 \varphi} \quad (18)$$

where  $\xi$  is the parametric latitude (Equation (19)),  $b$  is the semi-minor axis of the ellipsoid,  $p$  is the perpendicular distance from the rotational axis (Equation (20)) and  $\varepsilon$  (Equation (21)) is the second eccentricity.

$$\xi = \tan^{-1} \left[ \frac{aZ}{bP} \right] \quad (19)$$

$$p = \sqrt{X^2 + Y^2} \quad (20)$$

$$\varepsilon = \frac{e^2}{1 - e^2} \quad (21)$$

#### *Step 5: Fuse TLS Results into RBFNN (Hybrid model)*

The reverse conversion in Step 4 was necessary in order to select the input variables that produces the best results when the RBFNN was trained. This is important because it has been found that the appropriate input parameters used have influence on the prediction accuracy of the ANN model (Dreiseitl and Ohno-Machado 2002; Ismail, Shabri, & Samsudin, 2012). In the light of that, several input parameters were tried and tested to determine the one that can produce the best transformation results. Firstly,  $(X, Y, Z)_{TLS\ NEW}$  obtained in Step 3 was used as the input data and its corresponding  $(X, Y, Z)_{WAR}$  was used as the output data in the RBFNN training. In the second scenario,  $(\varphi, \lambda, h)_{TLS\ NEW\ 1}$  obtained in Step 4 was used as the input data and  $(\varphi, \lambda, h)_{WAR}$  as the output data. In the third scenario, The RBFNN was trained using  $(\varphi, \lambda)_{TLS\ NEW\ 1}$  obtained in Step 4 as the input variables and  $(\varphi, \lambda)_{WAR}$  as the output variable. It was found that using the third case yielded better fusion of TLS and RBFNN results. Thus, the hybrid model was formed by using the TLS transformed coordinates as the input data with its corresponding coordinates in the Ghana War Office 1926 as the output data. When the training process was over, the hybrid calculation model for coordinate transformation in the study area was developed.

#### *Step 6: Transforming Coordinates with Hybrid Model (TLS-RBFNN)*

For any position in the study area, when its transformed geodetic coordinates are computed using the TLS algorithm (Steps 1 to 4), then its improved transformed coordinates can be calculated using the TLS-RBFNN developed in Step 5. In furtherance of this, the five testing points were used to test the capability of the TLS-RBFNN model developed. In that case,  $(\varphi, \lambda)_{TLS\ TEST\ 1}$  obtained in Step 4 was used as the input data in the optimum trained hybrid model and its corresponding known coordinates in the War Office 1926 denoted as  $(\varphi, \lambda)_{WAR\ TEST}$  served as the target output. The new predicted output from the optimum trained hybrid model is represented as  $(\varphi, \lambda)_{WAR\ NEW}$ . The  $(\varphi, \lambda)_{WAR\ NEW}$  geodetic coordinates were then projected onto the Transverse Mercator 1° NW to obtain 2D projected grid coordinates in Easting (E) and Northing (N) using equations in Dzidefo (2011). The computed projected grid coordinates were then compared with the known grid coordinates for

statistical analysis. The map projection conducted was important because Ghana uses the 2D projected grid coordinate system for its surveying and mapping related activities.

#### *Step 7: Statistical Analysis*

In order to check the efficiency of TLS, RBFNN and TLS-RBFNN, residuals between the known and computed projected grid coordinates were estimated. Statistical evaluation metric presented in Section 4 were then used to quantify these residuals generated for results interpretation.

#### **Model Performance Criteria**

Performance criteria indicators (PCIs) such as Horizontal Error (HE), Root Mean Square Horizontal Error (RMSHE), Mean Horizontal Error (MHE), Standard deviation (SD), Maximum Error (Max Error) and Minimum Error (Min Error) were used to check the adequacy of the methods applied. The mathematical representations (Ziggah *et al.*, 2019a) of the various PCIs are given by Equations (22) to (27).

$$HE = \sqrt{(E_{i_i} - E_{o_i})^2 + (N_{i_i} - N_{o_i})^2} = \sqrt{\Delta E^2 + \Delta N^2} \quad (22)$$

$$RMSHE = \sqrt{\frac{\sum_{i=1}^n (HE_i)^2}{n}} \quad (23)$$

$$MHE = \frac{1}{n} \sum_{i=1}^n HE_i \quad (24)$$

$$SD = \sqrt{\frac{1}{n-1} \sum_{i=1}^n (HE - \overline{HE})^2} \quad (25)$$

$$\text{Max HE} = \max (HE_i)_{i=1}^n \quad (26)$$

$$\text{Min HE} = \min (HE_i)_{i=1}^n \quad (27)$$

where  $n$  is the total number of test data used,  $E_i$  and  $N_i$  represent the known Easting and Northing grid coordinates while  $E_{o_i}$  and  $N_{o_i}$  are the computed grid coordinates given by the TLS, RBFNN and TLS-RBFNN, respectively.  $\overline{HE}$  is the average value of the horizontal error.

## RESULTS AND DISCUSSION

### Model Performance Analysis

The RBFNN model which gave the optimum results was [2-14-2]. Thus, 2 inputs consisting of  $(\varphi_{WGS84}, \lambda_{WGS84})$ , 14 hidden neurons and  $(\varphi_{WAR}, \lambda_{WAR})$  as the 2 outputs. The optimum TLS-RBFNN model comprises [2-14-2]. That is,  $(\varphi, \lambda)_{TLS\ NEW\ 1}$  is the 2 inputs data, 14 hidden neurons in the hidden layer and  $(\varphi_{WAR}, \lambda_{WAR})$  as the 2 outputs. In this study, the criterion to determine the optimum RBFNN and TLS-RBFNN model was based on the concept of ANN generalisation. It is a well-known fact that generalisation provides a more convincing estimate on the validity of ANN models (Urolagin, Prema, & Subba Reddy, 2011). That is, the ability of ANN model to perform well when untrained data is presented to the network. To achieve this, the Mean Square Error (MSE) criterion was employed. That is, the model structure that produced the least MSE when the test data was fed into the RBFNN and TLS-RBFNN trained models was selected as the optimum model. For the TLS, the derived transformation parameters and their respective standard deviations of the 14 common points for transforming WGS84 coordinates to War Office 1926 datum are presented in Table 1.

**Table 1** Total Least Squares Estimated Transformation Parameters

Parameter	Value	SD
Tx (m)	-153.0127	11.6995
Ty (m)	63.7693	22.4533

Tz (m)	368.0575	21.1464
Rx (rad)	-1.07E-06	1.86E-06
Ry (rad)	-6.39E-06	3.32E-06
Rz (rad)	4.84E-06	3.50E-06
S (ppm)	-7.49E-06	1.82E-06

Analysis of Table 2 shows the coordinate differences ( $\Delta E$ ,  $\Delta N$ ) between the known and computed projected grid coordinates from TLS, RBFNN and TLS-RBFNN, respectively.

**Table 2** Deviation of transformed test coordinates from existing coordinates

Test Point	TLS			RBFNN			TLS-RBFNN		
	$\Delta E(m)$	$\Delta N(m)$	HE (m)	$\Delta E(m)$	$\Delta N(m)$	HE (m)	$\Delta E(m)$	$\Delta N(m)$	HE (m)
T1	0.0793	1.7516	1.7534	0.2608	1.7445	1.7638	-0.2013	0.0387	0.2050
T2	0.3799	-0.3783	0.5361	0.5529	-0.0397	0.5543	-0.1618	0.4065	0.4376
T3	-0.7647	0.0937	0.7704	-0.6216	-0.4831	0.7873	0.2997	0.5741	0.6476
T4	-1.5285	-0.1834	1.5394	-0.8093	-0.3765	0.8926	0.0483	-0.3246	0.3282
T5	-1.2642	-1.4062	1.8909	-0.7940	-0.5080	0.9426	0.0580	1.1290	1.1305
<b>Mean</b>	-0.6196	-0.0245	1.2980	-0.2822	0.0674	0.9881	0.0086	0.3647	0.5498
<b>SD</b>	0.8292	1.1432	0.6074	0.6417	0.9559	0.4587	0.2012	0.5503	0.3631

A careful study of the results in Table 2 reveals how much the computed Easting and Northing coordinates produced by TLS, RBFNN and TLS-RBFNN of the test points vary in conjunction with the ideal residual threshold value of zero. These values ( $\Delta E$ ,  $\Delta N$ ) give a better indication on the amount of discrepancies in the TLS, RBFNN and TLS-RBFNN computed coordinates compared to the known coordinates by way of errors. From Table 2, there is quantitative evidence of improvement of the TLS and RBFNN results by TLS-RBFNN. This could mean that the calibration capability of TLS-RBFNN architecture was better for the given training data and **that** has greater learning abilities compared to independently applying TLS and RBFNN to the data. In continuance of this, the result in

Table 2 shows that the hybrid TLS-RBFNN model could generalise better with the test data than TLS and RBFNN. The SD values (Table 2) of the coordinate differences estimated signify a practical expression for the precision of the computed coordinates given by TLS, RBFNN and TLS-RBFNN, respectively. In Table 2, it can be seen that TLS-RBFNN had the least SD values indicating the limit of the error bound by which every value within the computed test coordinates values varies from the most probable value.

Table 3 provides summary performance statistics of the total horizontal errors for TLS, RBFNN and TLS-RBFNN, respectively. From Table 3, it can be noticed that the hybrid TLS-RBFNN showed better results as compared to the other two techniques. Thus, TLS-RBFNN showed an improved percentage values of 76.870 and 43.140 in the transformation accuracy (RMSHE) for TLS and RBFNN. In terms of MHE, TLS-RBFNN improved TLS and RBFNN results by 74.820 and 43.830% respectively. For the maximum horizontal error, 76.040 and 63.330% were the percentage improvements by TLS-RBFNN. In the case of the minimum horizontal error, 33.110 and 34.930% were the improved percentage values. The inference made here is that TLS and RBFNN could not model the uncertainties of coordinates related to War Office 1926 and WGS84 in an effective way as compared to the TLS-RBFNN. On the basis of the SD values, TLS-RBFNN improved TLS and RBFNN by 24.430 and 9.560% (Table 3) with regards to the transformation precision.

**Table 3** Total Horizontal Residuals of the Coordinate Differences Using the Three Methods

PCI	TLS (m)	RBFNN (m)	TLS-RBFNN (m)	Improvement for TLS (%)	Improvement for RBFNN (%)
RMSHE	1.4072	1.0699	0.6385	76.870	43.140
MHE	1.2980	0.9881	0.5498	74.820	43.830
Max HE	1.8909	1.7638	1.1305	76.040	63.330
Min HE	0.5361	0.5543	0.2050	33.110	34.930
SD	0.6074	0.4587	0.3631	24.430	9.560

### Model Selection Criterion

---

Assessing the Integration of Total Least Squares and Radial Basis Function Neural Network for Coordinate Transformation (11905)

Bernard Kumi-Boateng and Joseph Edem Vigbedor (Ghana)

FIG Working Week 2023

Protecting Our World, Conquering New Frontiers

Orlando, Florida, USA, 28 May–1 June 2023

To select the best performing model, the Bayesian Information Criterion (BIC) was explored. In this study, the HE values for each of the five test points were used to calculate the BIC value. **The BIC was chosen because it tends to favour models with fewer parameters compared to other information criteria because its penalty term is smaller (Burnham and Anderson, 2002).** The BIC is represented mathematically (Equation (28)) as

$$BIC = n \times \ln\left(\frac{SSE}{n}\right) + K \times \ln(n) \quad (28)$$

where  $n$  denotes the number of observations,  $SSE$  is the sum of squares of the residuals and  $K$  is defined as the penalty term which corresponds to the number of unknown parameters in a coordinate transformation model (Table 4). Thus, the SSE is acting as an optimality criterion to aid in the BIC model selection. Therefore, a model is selected as the most suitable candidate model if it gives the least estimated BIC value. With this in mind, it can be inferred from Table 4 that TLS-RBFNN is more feasible for transforming coordinates between WGS84 datum and War Office 1926 datum.

**Table 4** Bayesian Information Criterion Model Selection Results

Method	K parameter	BIC Value
TLS	7	14.6817
RBFNN	2	3.8944
TLS-RBFNN	2	-1.2669

### Coordinate Transformation Using Entire Dataset

Ghana GNSS reference station network at the moment covers only the Mid-Southern parts with expansion to cover the North and the whole country is yet to be done. Therefore, due to limited data availability in the study area (Ghana), a particular cross-validation technique was adopted to test the potential of the already determined optimal models of TLS, RBFNN and TLS-RBFNN using the entire dataset. In this approach, the testing data of five points were swapped in the optimized models with the 19 co-located points. Thus, the 19 points were applied as the testing data in the optimum RBFNN and TLS-RBFNN structure of [2-14-2] which has already been formed using the training data of 14 co-located points. Similarly, the

transformation parameters determined using the TLS approach were also used to transform the whole dataset.

Mathematically, the test results produced using the entire dataset will give a better indication of all possible variations in the data and that will enable the model developer and users to ascertain the strength and generalisation capability of the developed models should the data size increase in the study area. In addition, it will provide a realistic estimate of the predictive potential of the TLS, RBFNN and TLS-RBFNN across the entire study area. This procedure has been adopted in several studies in order to check the overall generalisation of ANNs (Konaté, Pan, Khan, & Ziggah, 2015; Ziggah *et al.*, 2016b). The entire data testing results achieved by TLS, RBFNN and TLS-RBFNN are presented in Table 5.

**Table 5** Deviation of Transformed Test Coordinates Using the Whole Data set

Point	TLS			RBFNN			TLS-RBFNN		
	$\Delta E$ (m)	$\Delta N$ (m)	HE(m)	$\Delta E$ (m)	$\Delta N$ (m)	HE(m)	$\Delta E$ (m)	$\Delta N$ (m)	HE(m)
T1	-0.3692	1.1937	1.2495	-0.4021	0.8442	0.9351	-0.1086	-0.4933	0.5051
T2	-0.1522	0.9330	0.9454	-0.2589	0.8414	0.8803	-0.0110	0.3605	0.3607
T3	0.4910	-1.6776	1.7479	0.2246	-1.1899	1.2109	-0.0064	-0.0365	0.0371
T4	-0.6727	-0.6522	0.9370	-0.5209	-1.3907	1.4851	-0.0978	-0.2829	0.2993
T5	0.0600	-0.9153	0.9173	-0.2790	-0.4701	0.5466	-0.0894	-0.6217	0.6281
T6	0.2516	0.5738	0.6265	0.0827	0.8848	0.8886	0.2740	0.9442	0.9831
T7	0.3772	-0.1226	0.3966	0.2504	-0.1123	0.2744	0.0615	0.5202	0.5238
T8	0.3940	-0.3777	0.5458	0.1609	-0.1136	0.1969	0.3702	0.1237	0.3903
T9	-0.4205	-0.4637	0.6260	-0.7729	-0.1023	0.7796	-0.6297	-0.4714	0.7866
T10	0.3165	0.7873	0.8485	0.3901	0.0289	0.3912	-0.0109	0.3524	0.3526
T11	-0.3867	0.5759	0.6937	-0.5904	0.1356	0.6057	0.1550	0.2527	0.2964
T12	0.6269	0.0195	0.6272	0.3452	-0.1077	0.3616	0.3119	-0.5031	0.5919
T13	-0.4063	0.3972	0.5682	-0.6027	0.3222	0.6834	-0.2460	-0.1002	0.2656
T14	-0.1628	-0.2977	0.3393	-0.4740	0.1553	0.4988	0.0473	-0.0497	0.0686
T15	0.0793	1.7516	1.7534	0.2608	1.7445	1.7638	-0.1920	-1.5900	1.6016

Assessing the Integration of Total Least Squares and Radial Basis Function Neural Network for Coordinate Transformation (11905)

Bernard Kumi-Boateng and Joseph Edem Vigbedor (Ghana)

FIG Working Week 2023

Protecting Our World, Conquering New Frontiers

Orlando, Florida, USA, 28 May–1 June 2023

T16	0.3799	-0.3783	0.5361	0.5529	-0.0397	0.5543	-0.1171	0.7646	0.7735
T17	-0.7647	0.0937	0.7704	-0.6216	-0.4831	0.7873	0.3221	0.5301	0.6203
T18	-1.5285	-0.1834	1.5394	-0.8093	-0.3765	0.8926	-0.0032	0.0248	0.0251
T19	-1.2642	-1.4062	1.8909	-0.7940	-0.5080	0.9426	0.0570	1.1290	1.1304
<b>SD</b>	<b>0.5952</b>	<b>0.8661</b>	<b>0.4816</b>	<b>0.4589</b>	<b>0.7321</b>	<b>0.4001</b>	<b>0.2337</b>	<b>0.6379</b>	<b>0.3964</b>

Judging from the outcomes in Table 5, it can be inferred on the basis of the HE values that TLS-RBFNN model achieved satisfactory testing results than RBFNN and TLS. This demonstrates that TLS-RBFNN has good generalisation capabilities across the entire study area. Hence, it can evidently be stated that the TLS-RBFNN computed projected grid coordinates (testing outputs) are in better agreement to the known projected grid coordinates.

In addition, the lowest SD values (Table 5) obtained by TLS-RBFNN revealed its generalisation superiority to the other methods. These SD values show the range of precision of the TLS, RBFNN and TLS-RBFNN computed projected grid coordinates on a normal distribution curve. In line with this, it can be stated that the TLS-RBFNN transformation results are more precise and accurate than the TLS and RBFNN. Intuitive interpretation of Figure 4 shows that the TLS-RBFNN generalised better across the entire data for the study area than the TLS and RBFNN, respectively.

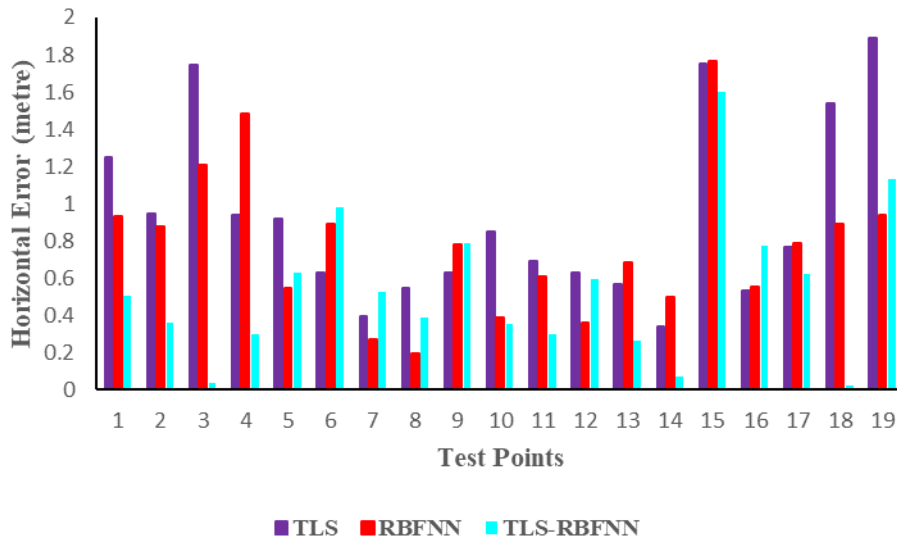


**Figure 4.** Horizontal Displacement of the Entire Data (testing data)

As evident from Table 6, the TLS-RBFNN had a transformation accuracy of 0.6628 m while 1.0362 m and 0.8652 m were respectively produced by TLS and RBFNN. In percentage wise, the TLS and RBFNN transformation accuracies were improved by 37.34 and 20.24, respectively. These signify the degree at which the hybrid TLS-RBFNN model could improve the transformation results in the study area rather than independently applying TLS and RBFNN. Taking into account the average dispersion of horizontal errors (MHE), it can be seen that when TLS-RBFNN was applied the TLS and RBFNN results were improved by 38.52% and 23.36%. The maximum and minimum HE (Table 6), on the other hand, signify the quality of the results produced by the three methods with respect to the range of error achievable when TLS, RBFNN and TLS-RBFNN were applied in the study area. An observation from Table 6 shows that independently applying TLS and RBFNN in the study area will achieve maximum HE values of 1.8909 m and 1.7638 m with 0.3393 m and 0.1969 m being the minimum. However, should the TLS-RBFNN be applied, TLS and RBFNN results could be improved by 28.93% and 16.22% for their maximum HE. In relation to minimum HE, 31.42% and 17.18% could be obtained. On account of the SD calculated values (Table 6), it could be seen that a transformation precision of 0.3964 m was achieved by TLS-RBFNN while 0.4816 m and 0.4001 m were realised by TLS and RBFNN respectively. The

TLS-RBFNN results indicate percentage improvement of TLS and RBFNN results by 8.52% and 0.37%.

**Table 6** Total Horizontal Residuals using the Entire data

<b>PCI</b>	<b>TLS (m)</b>	<b>RBFNN(m)</b>	<b>TLS-RBFNN(m)</b>	<b>Improvement for TLS (%)</b>	<b>Improvement for RBFNN (%)</b>
RMSHE	1.0362	0.8652	0.6628	37.340	20.240
MHE	0.9242	0.7726	0.539	38.520	23.360
Max HE	1.8909	1.7638	1.6016	28.930	16.220
Min HE	0.3393	0.1969	0.0251	31.420	17.180
SD	0.4816	0.4001	0.3964	8.520	0.370

The computed BIC values (Table 7) based on the HE (Table 5) of the entire data set showed that the combination of TLS and RBFNN had a better capability of producing improved transformation results than when they are separately applied. This is because among the three methods TLS-RBFNN had the least BIC value and thus was selected as the better technique over TLS and RBFNN, respectively. Hence, on the basis of the quantitative analyses presented in this study, it can logically be stated that the potential of the hybrid TLS-RBFNN approach in the coordinate transformation process for Ghana geodetic reference network has been duly investigated.

**Table 7** Bayesian Information Criterion Model Selection Using Whole Data

<b>Method</b>	<b>K Parameter</b>	<b>BIC Value</b>
TLS	7	12.6190
RBFNN	2	-2.2856
TLS-RBFNN	2	-12.4093

## **CONCLUSIONS AND RECOMMENDATION**

An experiment to combine TLS and RBFNN in coordinate transformation process has been presented. This hybrid TLS-RBFNN approach was applied to data in Ghana geodetic reference network. The major point is to test the potential of such integrated approach in transforming coordinates from WGS84 to War Office 1926 in Ghana geodetic reference network. The quantitative analyses revealed that the hybrid TLS-RBFNN offered better transformation results compared to TLS and RBFNN. This clearly indicates that the TLS-RBFNN can modify its behaviour to improve its learning ability and to generalise well to unseen data (test data). In this study, the TLS-RBFNN approach gave overall transformation accuracy (RMSHE) of 0.6628 m while 1.0362 m and 0.8652 m were respectively achieved by TLS and RBFNN for the entire data test points. In terms of percentage, the obtained values for TLS and RBFNN were improved by TLS-RBFNN by 37.340% and 20.240%. Similar performance enhancement were observed for the transformation precision (SD values), maximum and minimum recorded horizontal errors as well as the average horizontal error (MHE). On the strength of these transformation accuracies obtained in this study, it can be stated that the hybrid approach (TLS-RBFNN) results are logical and related to the legal regulations set by the Ghana Survey and Mapping Division of Lands Commission for cadastral applications and plan production. To conclude, it must be emphasised that the idea behind this study is not to take away the significance of the classical transformation models but to show from a practical perspective how RBFNN can be more effective in solving coordinate transformation problems when combined with the classical approach. This study, therefore, has demonstrated the potential and the resulting consequences of using the TLS integrated with RBFNN than applying the TLS and RBFNN independently in coordinate transformation process within Ghana geodetic reference network. Finally, future research works will focus on generalising the proposed hybrid approach across the entire country (Ghana) with more data availability upon completion of the GNSS reference stations in the near future. **It is also suggested that such works can be replicated in countries that have similar geodetic network infrastructure like Ghana. Additionally, it is also recommended that other hybrid models of TLS and artificial intelligence methods must be carried out to help select the best performing hybrid transformation model for Ghana.**

## ACKNOWLEDGEMENT

The authors wish to thank the Ghana Survey and Mapping Division of Lands Commission for making the data available to do this work.

**Competing Interest:** Authors declare no conflict of interest.

## REFERENCES

Akyilmaz, O. (2007). Total least squares solution of coordinate transformation. *Survey Review*, 39(303), 68-80.

Applebaum, L.T. (1982). Geodetic datum transformation by multiple regression equations. In: Peat, P.R., ed. *Third International Geodetic Symposium on Satellite Doppler Positioning*, Las Cruces, New Mexico, New Mexico State University (207-223).

Ayer, J. (2008). Transformation Models and Procedures for Framework Integration of the Ghana National Geodetic Network. *The Ghana Surveyor*, 1(2), 52–58.

Ayer, J., & Fosu, C. (2008). Map coordinates referencing and the use of GPS datasets in Ghana. *Journal of Science and Technology*, 28(1), 116-127.

Badekas, J. (1969). Investigations related to the establishment of a World Geodetic System. *Technical Report*, The Ohio State University, Dept. of Geodetic Science, Columbus, Ohio State, USA, (1-191).

Bowring, B.R. (1976). Transformation from spatial to geographical coordinates. *Survey Review*, 23(181), 323–327.

Broomhead, D.S., & Lowe, D. (1988). Multivariate functional interpolation and adaptive networks. *Complex Systems*, 2, 321-355.

---

Assessing the Integration of Total Least Squares and Radial Basis Function Neural Network for Coordinate Transformation (11905)  
Bernard Kumi-Boateng and Joseph Edem Vigbedor (Ghana)

FIG Working Week 2023  
Protecting Our World, Conquering New Frontiers  
Orlando, Florida, USA, 28 May–1 June 2023

Burnham, P.K., & Anderson, R.D. (2002). *Model Selection and Multimodel Inference: A Practical Information-Theoretic Approach* (pp.1-454), Springer-Verlag New York, Inc, USA.

Bursa, M. (1962). The theory of the determination of the nonparallelism of the minor axis of the reference ellipsoid, Polar axis of the Earth, and initial astronomical and geodetic meridians from observation of artificial Earth satellites. *Studia Geophysica et Geodaetica*, 6(2), 209-214.

Collier, P.A., Argeseanu, V., & Leahy, F. (1998). Distortion Modelling and the Transition to GDA94. *Australian Surveyor*, 43(1), 29-40.

Deyfrus, G. (2005). *Neural networks: methodology and applications* (pp.1-490). Springer-Verlag, Berlin, Germany.

Dreiseitl, S., & Ohno-Machado, L. (2002). Logistic regression and artificial neural network classification models: a methodology review. *Journal of Biomedical Informatics*, 35(5), 352-359.

Dzidefo, A. (2011). *Determination of Transformation Parameters between the World Geodetic System 1984 and the Ghana Geodetic Network* (Master's Thesis), Department of Civil and Geomatic Engineering, KNUST, Kumasi, Ghana.

Featherstone, W.E. (1997). A Comparison of Existing Co-ordinate Transformation Models and Parameters in Australia. *Cartography*, 26 (1), 13-26.

Felus, Y.A., & Schaffrin, B. (2005). Performing Similarity Transformations using the Error-in-Variable Model. In *ASPRS Annual Conference, Geospatial Goes Global: From Your Neighbourhood to the Whole Planet*, Baltimore, Maryland (1-8).

Fraser, C.S., & Yamakawa, T. (2004). Insights into the Affine Model for High-Resolution Satellite Sensor Orientation. *ISPRS Journal of Photogrammetry and Remote Sensing*, 58, 275-288.

Ghorbani, M.A., Khatibi, R., Fazeli Fard, M.H., Naghipour, L., & Makarynsky, O. (2016). Short-term wind speed predictions with machine learning techniques. *Meteorology and Atmospheric Physics*, 128(1), 57-72.

Golub, G.H., & Van Loan, C.F. (1980). An analysis of the total least squares problem. *Journal of Numerical Analysis*, 17(6), 883-893.

Grafarend, E.W., & Awange, J.L. (2003). Nonlinear analysis of the three-dimensional datum transformation [conformal group  $C7(3)$ ]. *Journal of Geodesy*, 77, 66-76.

Grgić, M., Varga, M., & Basic, T. (2015). Empirical research of interpolation methods in distortion modelling for the coordinate transformation between local and global geodetic datums. *Journal of Surveying Engineering*, 142(2), 66-76.

Gullu, M., & Narin, O.G. (2019). Georeferencing of the Nile River in Piri Reis 1521 map using artificial neural network method. *Acta Geodaetica et Geophysica*, 54(3), 387-401.

Hofmann-Wellenhof, B., & Moritz, H. (2006). *Physical Geodesy* (pp. 1-402) 2nd Edition, Springer Science & Business Media, Austria.

Huang, F.M., Wu, P., & Ziggah, Y.Y. (2016). GPS monitoring landslide deformation signal processing using time-series model. *International Journal of Signal Processing, Image Processing and Pattern Recognition*, 9 (3), 321-332.

Ismail, S., Shabri, A., & Samsudin, R. (2012). A hybrid model of self-organizing maps and least square support vector machine for river flow forecasting. *Hydrology and Earth System Sciences*, 16(11), 4417-4433.

Jain, T., Singh, S.N., & Srivastava, S.C. (2011). Fast static available transfer capability determination using radial basis function neural network. *Applied Soft Computing*, 11(2), 2756-2764.

Kaftan, I., Salk, M., & Senol, Y. (2011). Evaluation of gravity data by using artificial neural networks case study: Seferihisar geothermal area (Western Turkey). *Journal of Applied Geophysics*, 75(4), 711-718.

Konaté, A.A., Pan, H., Khan, N., & Ziggah, Y.Y. (2015). Prediction of porosity in crystalline rocks using artificial neural networks: an example from the Chinese continental scientific drilling main hole. *Studia Geophysica et Geodaetica*, 59(1), 113-136.

Kumi-Boateng, B., & Ziggah, Y.Y. (2017). Horizontal coordinate transformation using artificial neural network technology-A case study of Ghana geodetic reference network. *Journal of Geomatics*, 11(1), 1-11.

Lei, Y., Zhao, D., & Cai, H. (2015). Prediction of length-of-day using extreme learning machine. *Geodesy and Geodynamics*, 6(2), 151-159.

Liao, D.C., Wang, Q.J., Zhou, Y.H., Liao, X.H., & Huang, C.L. (2012). Long-term prediction of the earth orientation parameters by the artificial neural network technique. *Journal of Geodynamics*, 62, 87-92.

Lippus, J. (2004). Transformation of coordinates using piecewise conformal mapping. *Journal of Geodesy*, 78, 40-46.

Markovsky, I., & Van Huffel, S. (2007). Overview of total least-squares. *Signal Processing*, 87 (10), 2283-2302.

Molodensky, M.S., Yeremeyev, V., & Yurkina, M. (1962). Methods for study of the external Gravitational Field and Figure of the Earth. *Technical report Office of Technical services*, US Dept. of Commerce, Israel Program for Scientific Translations, Jerusalem, Israel (Russian), 1-248.

Mugnier, J.C. (2000). OGP-coordinate conversions and transformations including formulae, COLUMN, Grids and Datums. The Republic of Ghana. *Photogrammetric Engineering and Remote Sensing*, 695-697.

Newsome, G.G., & Harvey, B.R. (2003). GPS Coordinate Transformation Parameters for Jamaica. *Survey Review*, 37(289), 218-234.

Okwuashi, O., & Eyoh, E. (2012). 3D coordinate transformation using total least squares. *Academic Research International*, 3 (1), 2223-9944.

Okwuashi, O., & Ndehedehe, C. (2015). Digital terrain model height estimation using support vector machine regression. *South African Journal of Science*, 111 (9-10), 01-05.

Poku-Gyamfi, Y. (2009). *Establishment of GPS Reference Network in Ghana*. (PhD Theses), Universitat der Bundeswehr Munchen, Germany.

Razin, M.R.G., & Voosoghi, B. (2017). Ionosphere tomography using wavelet neural network and particle swarm optimization training algorithm in Iranian case study. *GPS Solutions*, 21(3), 1301-1314.

Salim, A.M., Dwarakish, G.S., Liju, K.V., Thomas, J., Devi, G., & Rajeesh, R. (2015). Weekly prediction of tides using neural networks. *Procedia Engineering*, 116, 678-682.

Shen, Y.Z., Chen, Y., & Zheng, D.H. (2006). A quaternion-based geodetic datum transformation. *Journal of Geodesy*, 80, 233–239.

Soler, T., & Snay, R. (2003). Transforming positions and velocities between International Terrestrial Reference Frame of 2000 and North America Datum of 1983. *Journal of Surveying Engineering*, 130, 49-55.

Tierra, A.R., & De Freitas, S.R.C. (2005). Artificial Neural Network: A Powerful Tool for Predicting Gravity Anomaly from Sparse Data. *Gravity, Geoid and Space Missions, International Association of Geodesy Symposia* (208-213).

Tierra, A.R., De Freitas, S.R.C., & Guevara, P.M. (2009). Using an Artificial Neural Network to Transformation of Coordinates from PSAD56 to SIRGAS95. *Geodetic Reference Frames, International Association of Geodesy Symposia* (134,173-178).

Tiwari, M., Adamowski, J., & Adamowski, K. (2016). Water demand forecasting using extreme learning machines. *Journal of Water and Land Development*, 28(1), 37-52.

Urolagin, S., Prema, K.V., & Subba Reddy, N.V. (2011). Generalization Capability of Artificial Neural Network Incorporated with Pruning Method. *Advanced Computing, Networking and Security: International Conference, ADCONS 2011, Surathkal, India, December 16-18*, (7(135):171-178).

Van Huffel, S., & Vandewalle, J. (1991). *The Total Least Squares Problem – Computational Aspects and Analysis*, Frontiers in Applied Mathematics (pp. 1-302). Society for Industrial and Applied Mathematics, USA.

Varga, M., Grgić, M. & Bašić, T. (2017). Empirical comparison of the Geodetic Coordinate Transformation Models: a case study of Croatia. *Survey Review*, 49(352), 15-27.

Wang, W., & Yuan, H. (2018). A tidal level prediction approach based on BP neural network and cubic b-spline curve with knot insertion algorithm. *Mathematical Problems in Engineering*, 2018 Article ID 9835079(1-9).

Wolf, H. (1963). Geometric connection and reorientation of three-dimensional triangulation nets. *Bulletin Geodesique*, 68(1), 165-169.

Ziggah, Y.Y., & Laari, P.B. (2018). Application of Multivariate Adaptive Regression Spline (MARS) Approach for 2D Coordinate Transformation. *Ghana journal of technology*, 2(2), 50-62.

Ziggah, Y.Y., Youjian, H., Tierra, A.R., & Laari, P.B. (2019a). Coordinate transformation between global and local data based on artificial neural network with k-fold cross-validation in Ghana. *Earth Sciences Research Journal*, 23(1), 67-77.

Ziggah, Y.Y., Hu, Y., Issaka, Y., & Laari, P.B. (2019b). Least squares support vector machine model for coordinate transformation. *Geodesy and Cartography*, 45(1), 16-27.

Ziggah, Y.Y., Issaka, Y., Laari, P.B., & Hui, Z. (2018). 2D cadastral coordinate transformation using extreme learning machine technique. *Geodesy and Cartography*, 67(2), 321-343.

Ziggah, Y.Y., Youjian, H., Laari, P.B., & Hui, Z. (2017). Novel approach to improve geocentric translation model performance using artificial neural network technology. *Boletim de Ciências Geodésicas*, 23(1), 213-233.

Ziggah, Y.Y., Youjian, H., Tierra, A., Konaté, A.A., & Hui, Z. (2016a). Performance evaluation of artificial neural networks for planimetric coordinate transformation-a case study, Ghana. *Arabian Journal of Geosciences*, 9(17), 698, 1-16.

Ziggah, Y.Y., Youjian, H., Yu, X., & Laari, P. B. (2016b). Capability of Artificial Neural Network for Forward Conversion of Geodetic Coordinates ( $\phi, \lambda, h$ ) to Cartesian Coordinates ( $X, Y, Z$ ). *Mathematical Geosciences*, 48, 687-721.

---

Assessing the Integration of Total Least Squares and Radial Basis Function Neural Network for Coordinate Transformation (11905)  
Bernard Kumi-Boateng and Joseph Edem Vigbedor (Ghana)

FIG Working Week 2023  
Protecting Our World, Conquering New Frontiers  
Orlando, Florida, USA, 28 May–1 June 2023